SMALL ANGLE RAYLEIGH SCATTERING OF Co^{60} GAMMA RAYS

S. A. BEL'SKIĬ and S. V. STARODUBTSEV

Leningrad Physico-Technical Institute, Academy of Sciences, U.S.S.R.

Submitted to JETP editor May 22, 1959

J. Exptl. Theoret. Phys. (U.S.S.R.) **37**, 983-990 (October, 1959)

The integral cross sections for the Rayleigh scattering of Co^{60} γ rays from U, Pb, W, Ta, Sn, Cu and Ni have been measured for the angular intervals 15′ to 1°00′ and 15′ to 2°30′. The results confirm the prediction of the Debye-Franz theory that at small angles the cross section for Rayleigh scattering is proportional to the square of the atomic number of the scatterer. It is further shown that at the angles considered, the experimental values of the Rayleigh cross sections are greater than the theoretically predicted ones, and that with decreasing Z the angular dependence of the cross section becomes more pronounced than that indicated by theory.

1. INTRODUCTION

FOR energies of order 1 Mev, γ rays can interact elastically with matter through Rayleigh scattering from bound electrons, resonance scattering from nuclei, Thomson scattering from nuclei as charges, and potential scattering with the formation of virtual pairs in the field of the nucleus (the so-called Delbrück scattering). Rayleigh scattering at x-ray frequencies has long been known, but the other effects, together with Rayleigh scattering at high γ-ray energies, has not been studied experimentally.

There are two fundamental difficulties in the experimental investigation of elastic scattering of γ rays of about 1 Mev energy. The first is that the cross section for elastic scattering is much less than that for inelastic Compton scattering. The second difficulty is that the elastically scattered photons are masked by a hard component of the bremsstrahlung from Compton and photo-electrons, together with radiation from the annihilation of positrons. Using scintillation techniques, the inelastic Compton component can be discriminated against at large angles, but the hard bremsstrahlung remains troublesome.

Of the four processes for elastic scattering, Rayleigh scattering has the biggest cross section. There are several reasons why an experimental study of Rayleigh scattering is of interest. According to the non-relativistic theory of Debye and Franz,[1,2] which is based on the Thomas-Fermi approximation to the distribution of electron charge in an atom, at large scattering angles the cross section is proportional to the cube of the atomic number of the scatterer. Bethe and Levinger[3] carried out relativistic calculations, using Dirac wave functions for the K electrons, and at large angles obtained somewhat lower cross sections than those predicted by Debye and Franz, and a variation of the cross section with atomic number given by $Z^8 - Z^{10}$. More exact relativistic calculations of the cross section for Rayleigh scattering, with several terms of the Born expansion into a sum over intermediate states being taken into account, have been carried out recently[4-7] for γ-ray energies 0.32, 0.64, 1.28 and 2.56 mc^2. At all angles the cross sections so obtained are lower than those given by the Debye-Franz theory and vary with the atomic number as Z^5.

In resonance scattering experiments, Rayleigh scattering gives rise to a background whose magnitude must be known before a reliable value for the resonance scattering cross section can be obtained. In recent years, resonance scattering has become one of the fundamental methods for measuring the lifetimes of excited states as short as 10^{-11} sec. The resonance scattering technique is useful in solving other important problems, too. Finally, although it has now become possible to measure Rayleigh scattering, the existence of Delbrück and Thomson scattering has not yet been demonstrated experimentally. Since these compete with Rayleigh scattering, it is important in studying them to have reliable theoretical and experimental data on the cross section and angular distribution of the Rayleigh scattering, together with its dependence on the energy of the γ rays and the atomic number of the scatterer.

Rayleigh scattering has a strong angular dependence, as predicted by theory. At large angles, the cross section for Rayleigh scattering is several orders of magnitude less than that for Compton scattering, while at small angles it is considerably larger than Compton scattering. Hence there are two convenient regions for experimental studies of Rayleigh scattering: 1) large angles, where the soft Compton component can be discriminated against; 2) small angles, where Compton scattering is negligible compared to Rayleigh scattering.

There have been a number of experiments carried out in recent years[8-17] at larger scattering angles (> 30°). These experiments measured the magnitude of the Rayleigh cross section, its angular dependence, and variation with Z, for γ-ray energies in the range 0.41 — 2.76 Mev. The results of various authors do not agree, which can be explained by the difficulty of allowing for the secondary hard component contained in the measured elastic scattering.

In the work now being reported we studied the Rayleigh scattering of Co^{60} rays at small angles (< 3°) and the behavior of the cross section as a function of the atomic number of the scatterer. The results are compared with the Debye-Franz theory.

2. THEORY

According to Debye,[1] the cross section for Rayleigh scattering on the electron cloud of an atom is, at x ray energies, given by the formula

$$\sigma = \frac{4\pi e^4 Z^2}{E_0^2}\left(\frac{\lambda}{b}\right)^2 \int_0^{b/\lambda} \left(\frac{A}{Z}\right)^2 u\,du, \tag{1}$$

where E_0 is the electron rest mass, λ is the γ-ray wavelength, Z the atomic number of the scatterer, $b = 5.9 \times 10^{-8} Z^{-1/3}$ cm, $u = (b/\lambda)\sin(\theta/2)$, and θ is the scattering angle. The electron structure factor $f = A/Z$ is determined by the expression

$$f = \int_0^{\infty} x^{-1/2}\varphi^{3/2}\frac{\sin ux}{u}\,dx, \tag{2}$$

where $\varphi(x)$ is the Fermi function, $x = r/a$ (r = distance from the nucleus, $a = b/4\pi$ is a characteristic radius). Debye carried out this integration graphically for the range $0 \le u \le 2\pi$. Franz[2] extended Debye's calculations to the range $u \ge 2\pi$, the function $f = A/Z$ being obtained in analytic form as a series

$$f = \frac{1}{u}\sqrt{\frac{\pi}{2u}}\left(1 - \frac{1.19}{u} + \cdots\right). \tag{3}$$

Over the Debye range $(0 \le u \le 2\pi)$, the value of the integral in (1) is 0.6, while over Franz' range $(2\pi \le u \le b/\lambda)$ it is $0.2 - \pi\lambda/2b$. Hence, the total cross section for Rayleigh scattering is

$$\sigma = 4\pi e^4 Z^2 E_0^{-2}(\lambda/b)^2(0.8 - \pi\lambda/2b). \tag{4}$$

The γ rays from Co^{60} have mean energy $\overline{E}_\gamma = 1.25$ Mev; for lead the cross section becomes $\sigma = 3.71 \times 10^{-25}$ cm^2. Since $0.6/[0.8 - \pi\lambda/2b] > 0.75$, more than 75% of the radiation will be scattered through an angle smaller than some angle θ_0.

From the relation $u = 2\pi = b/\lambda \sin(\theta_0/2)$ and for $E_\gamma = 1.25$ Mev we find, for lead, $\theta_0 \approx 5.3°$, while for aluminum $\theta_0 \approx 2.8°$. From this it is evident that Rayleigh scattering is predominantly through small angles. From (1) we can easily derive an expression for the differential cross section for Rayleigh scattering:

$$S(\theta) = (e^4 Z^2/2E_0^2)(A/Z)^2 = 3.971 \cdot 10^{-26} \cdot Z^2 (A/Z)^2. \tag{5}$$

For $\theta \to 0$ $((A/Z)^2 \to 1)$ the cross section for Rayleigh scattering is proportional to Z^2, and reaches a maximum, independent of the γ-ray energy, given by

$$S(\theta)_{max} = 3.971 \cdot 10^{-26} Z^2. \tag{6}$$

3. EXPERIMENTAL TECHNIQUE

Figure 1 shows a diagram of the experiment. The lead blocks Pb_1 — Pb_4 were arranged so that the holes through their centers (hole diameter 5 mm) were lined up. The Co^{60} source was a metal cylinder 10 mm long, diameter 5 mm, and had an activity 1.8 C. The detection system consisted of a scintillation counter with a NaI(Tl) crystal and an integral discriminator. The electronics operated stably, as indicated by the fact that over 12 — 15 hours the counting rate did not change by more than 2 or 3 statistical errors. The statistical error $\pm\sqrt{N}/N$ in a single measurement was ± 0.3%. As scatterers we used U, Pb, W, Ta, Sn, Cu, and Ni discs with diameter 25 mm and thickness $l_Z = 2/\mu_Z$, where μ_Z is the

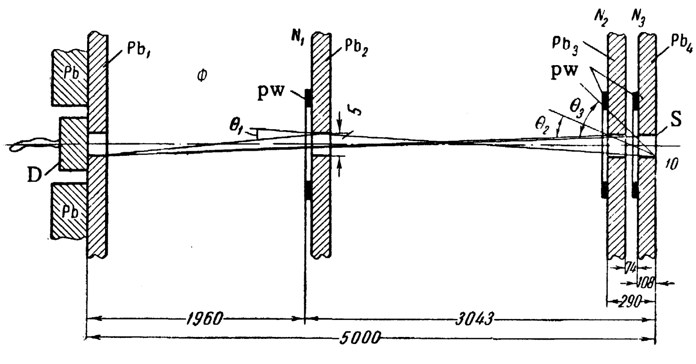

FIG. 1. Schematic diagram of the experimental set up. S – source, D – detector, pw – plexiglas washer for mounting the scatterers, θ_1, θ_2, and θ_3 – maximum scattering angles in the scatterer positions N_1, N_2, and N_3.

linear absorption coefficient for Co^{60} γ rays in the element used.

The Rayleigh-scattered radiation was measured as a small addition to a background provided by the direct beam. The magnitude of this increase depends on the solid angles subtended by the scatterer at the source and detector and the corresponding linear angle θ_{max}. The number of scattered γ quanta is given by the formula

$$I_{sc} = I_{pri} N_a x \int_0^{\theta_{max}} 2\pi S(\theta) \sin\theta \, d\theta = I_{pri} N_a x \sigma_0(\theta_{max}), \quad (7)$$

where N_a is the number of atoms per cc in the scatterer, x is the thickness of the scatterer and $\sigma_0(\theta_{max})$ is the scattering cross section for the interval 0° to θ_{max}.

It is clear that the amount of scattered radiation adding to the primary beam will depend on θ_{max}. The scatterer was successively placed in positions N_1, N_2, and N_3 (Fig. 1), in which positions the maximal scattering angles θ_1, θ_2, and θ_3 were as given in Table I. The maximal scattering angle θ_{max} depends on the maximal linear angles α_{max} and β_{max} subtended by the scatterer at the source and detector respectively. The angles β_3 and β_2 were each equal to 0° 04′, while β_1 was 0° 09′. The finite thickness of the scatterer gave rise to an uncertainty in the scattering angles, also shown in Table I.

Knowing the difference in γ counts between two positions of the scatterer, for instance N_1 and N_3, we can calculate the total scattering cross section $(\sigma_t)_1^3$ corresponding to the interval θ_1 to θ_3, the calculation being done according to the formula

$$(\sigma_t)_1^3 = (I_3 - I_1) / I_1 N_a x \, . \quad (8)$$

This method obviously is useful only for scattering processes whose differential cross section is sufficiently large at small angles. According to theory, in the angle interval 0 — 2° 30′ Rayleigh scattering of γ rays with $E_\gamma = 1.25$ Mev from heavy elements amounts to 1.5% of the direct beam.

4. COMPTON SCATTERING AND THE UNEQUAL CONTRIBUTIONS OF DIFFERENT SCATTERING ANGLES

The cross section determined from experiment using formula (8) is the sum of the Rayleigh cross section and all the other possible elastic and inelastic processes. We need correct only for Compton scattering because the contribution of all the other processes is negligibly small. At small angles, Compton and Rayleigh scattered quanta have practically the same energy and cannot be separated from each other. Hence the contribution of Compton scattering was computed theoretically. The Rayleigh cross section was then obtained as the difference between the total, measured, cross section and the contribution from Compton scattering: $(\sigma_R)_{exp} = (\sigma_t)_{exp} - (\sigma_C)_{theor}$. Theoretical values for the Rayleigh scattering were computed graphically. $S_R(\theta)$ was calculated from formula (5); the quantity $f(\theta) = 2\pi S_R(\theta) \sin\theta$ is shown in Fig. 2.

In calculating the theoretical Rayleigh and Comp-

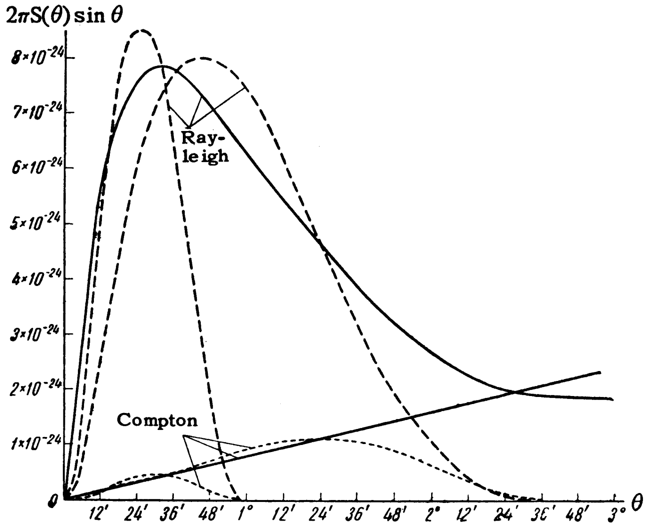

FIG. 2. Angular distribution of Rayleigh and Compton scattered γ rays from uranium. Solid curve – without taking the function $F(\varphi)$ into account; dashed curves – taking $F(\varphi)$ into account.

TABLE I. Maximal scattering angles

Z	α_3	θ_3	α_2	θ_2	α_1	θ_1
U	2°35′±12′	2°38′±12′	0°58′±2′	1°02′±2′	0°06′	0°15′
Pb	2°27′±19′	2°31′±19′	0°56′±2′	0°59′±2′	0°06′	0°15′
W	2°33′±13′	2°37′±13′	0°58′±2′	1°02′±2′	0°06′	0°15′
Ta	2°32′±14′	2°36′±14′	0°58′±2′	1°02′±2′	0°06′	0°15′
Sn	2°18′±29′	2°21′±29′	0°55′±5′	0°59′±5′	0°06′	0°15′
Cu	2°22′±25′	2°26′±25′	0°56′±4′	1°0′±4′	0°06′	0°15′
Ni	2°33′±24′	2°27′±24′	0°56′±4′	1°0′±4′	0°06′	0°15′

ton scattering cross sections, it is necessary to take account of the fact that different angles in the range 0° to θ_{max} contribute differently. The angular distribution function for particles emitted by the source and falling on the scatterer was, at our request, graciously furnished by Prof. G. A. Grinberg. This function was calculated for our special case, where $l \gg a$ (a being the diameter of the source and scatterer, while l is the distance between them) and has the form

$$F(\varphi) = (\varphi - \sin\varphi)\sin\varphi, \qquad (9)$$

where

$$\varphi = 2 \arccos (l\theta/2a).$$

From the plot of F vs. φ (Fig. 3) it follows that large scattering angles (small φ) and small scattering angles (large φ) contribute relatively little as compared with intermediate angles.

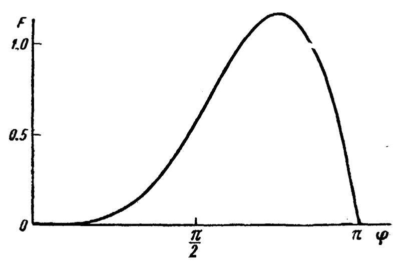

FIG. 3. Dependence of F on φ.

To correct for the unequal weight of different scattering angles, the function $f(\theta) = 2\pi S(\theta) \sin\theta$ for Rayleigh and Compton scattering was multiplied by the function $F(\varphi)$, for our values of the parameter $2a/l$ and the result integrated graphically. The product of these functions is shown in Fig. 2 for uranium. The theoretical values for the Rayleigh and Compton cross sections are shown in Table II, which also gives the corresponding cross sections without this correction (indicated by *).

5. MEASUREMENTS AND RESULTS

The measurements were carried out in the following way. The scatterer was placed first in one position, then in another, for example N_1 and N_3. In these positions, counts I_1 and I_3 were collected for five minutes each. In a single measurement, lasting five minutes, about 128,000 counts were collected, the background being about 500.

Several series of measurements were made on each scatterer; in a series, the counting rate for each position of the scatterer was determined 40 – 50 times. The arithmetic mean and mean square deviation of the differences in counting rates between the two scatterer positions was determined, the average being taken over several series, and the total scattering cross section determined from (8). The experimental data obtained are shown in Table II.

Figure 4 shows, in a semi-logarithmic plot, the theoretical and experimental dependence of the Rayleigh scattering cross section on the atomic number of the scatterer for the two intervals 15′ to 1°00′ and 15′ to 2°30′.

The following conclusions can be drawn from an analysis of the experimental data.

TABLE II

Angle Interval	$\theta_1 - \theta_3$					
Cross section in barns (per nucleus)	$(\sigma_P)_{exp}$	$(\sigma_C^*)_{theor}$	$(\sigma_C)_{theor}$	$(\sigma_R^*)_{theor}$	$(\sigma_R)_{theor}$	$(\sigma_R)_{exp}$
Uranium	0.217 ±0.011	0.047	0.027	0.198	0.166	0.180 ±0.011
Lead	0.175 ±0.012	0.038	0.021	0.144	0.120	0.154 ±0.012
Tungsten	0.126 ±0.011	0.036	0.020	0.112	0.095	0.106 ±0.010
Tantalum	0.151 ±0.009	0.036	0.020	0.107	0.090	0.131 ±0.009
Tin	0.0468 ±0.0028	0.0193	0.0111	0.0392	0.0318	0.0357 ±0.0028
Copper	0.0175 ±0.0012	0.0130	0.0069	0.0102	0.0085	0.0106 ±0.0012
Nickel	0.0131 ±0.0018	0.0128	0.0068	0.0093	0.0077	0.0062 ±0.0018

Angle Interval	$\theta_1 - \theta_2$					
Cross section in barns (per nucleus)	$(\sigma_P)_{exp}$	$(\sigma_C^*)_{theor}$	$(\sigma_C)_{theor}$	$(\sigma_R^*)_{theor}$	$(\sigma_R)_{theor}$	$(\sigma_R)_{exp}$
Uranium	0.085 ±0.010	0.007	0.004	0.098	0.069	0.081 ±0.010
Lead	0.074 ±0.050	0.006	0.003	0.072	0.050	0.071 ±0.005
Tungsten	0.058 ±0.013	0.006	0.003	0.058	0.041	0.055 ±0.013
Tantalum	0.083 ±0.014	0.006	0.003	0.055	0.040	0.080 ±0.014
Tin	0.0310 ±0.0012	0.0035	0.0015	0.0220	0.0152	0.0295 ±0.0012
Copper	0.0127 ±0.0015	0.0021	0.0010	0.0059	0.0045	0.0117 ±0.0015
Nickel	0.0053 ±0.0012	0.0020	0.0010	0.0055	0.0041	0.0043 ±0.0012

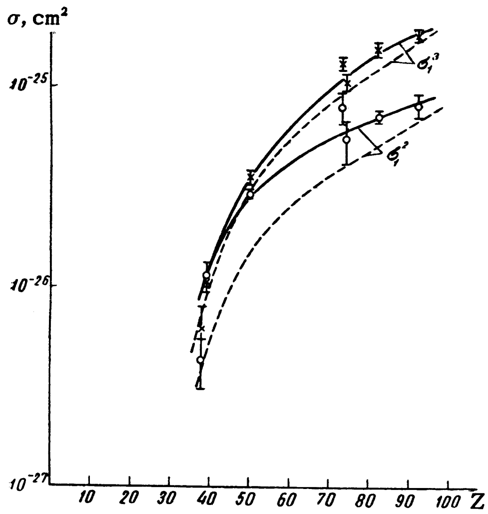

FIG. 4. Dependence of the Rayleigh scattering cross section on the atomic number of the scatterer. Dashed curve — theoretical, solid curve — experimental. × — experimental points for the angle interval θ_1–θ_3; o — for the interval θ_1–θ_2.

1. The cross section for Rayleigh scattering at small angles is greater than that predicted by the Debye-Franz theory. The experimental cross section becomes ever bigger than the theoretical one as the scattering angle decreases.

2. The experimental curves for σ_1^3 and σ_1^2 tend to come together as Z decreases. It follows that the experimental scattering cross section varies more strongly with decreasing Z than does the theoretical one. The experimental values of σ_1^3 and σ_1^2 coincide for Cu and Ni, i.e., for these elements we did not see Rayleigh scattering, within the limits of experimental error, at angles greater than 1°.

3. According to theory, about half the Rayleigh scattered radiation should be scattered through angles $\theta_1 = 15'$ to $\theta_2 = 2°30'$. The agreement between the general trend of the experimental and theoretical curves for σ_1^3 over this range of angles confirms the theoretical prediction that the Rayleigh scattering cross section should be proportional to the square of the atomic number of the scatterer.

The experimental points for Ta and Ni are anomalous. The scattering cross section for Ta turned out to be significantly greater than for its neighbor W, while for Ni the state of affairs is reversed, its cross section being markedly less than that for Cu. In this connection, it should be noted that a smooth variation of the angular distribution can be interrupted by diffraction effects. For Co^{60} γ rays, with energy $E_\gamma = 1.25$ Mev, the wave length is 10^{-10} cm, while interatomic distances are of order 10^{-8} cm. From the relation $n\lambda = 2d \sin\theta$ it follows that the first diffraction maximum will be at an angle 30′.

It should also be noted that elastic resonance scattering can occur in Ni; this will be out of phase with the Rayleigh scattering[17] and will compete with it. The observed decrease in the amplitude for elastic scattering can be explained by a strong resonance scattering peak at small angles, the mean differential cross section in the interval $\theta_1 - \theta_2$ being of order 1.37×10^{-24} cm²/sterad.

In conclusion, the authors would like to thank Prof. G. A. Grinberg for his help in making the calculations.

[1] P. Debye, Physik. Z. **31**, 348 (1930).
[2] W. Franz, Z. Physik **98**, 314 (1935).
[3] J. S. Levinger, Phys. Rev. **87**, 656 (1952).
[4] Brown, Peierls, and Woodward, Proc. Roy. Soc. (London) **A227**, 51 (1954).
[5] Brenner, Brown, and Woodward, Proc. Roy. Soc. (London) **A227**, 59 (1954).
[6] G. E. Brown and D. F. Mayers, Proc. Roy. Soc. (London) **A234**, 387 (1956).
[7] G. E. Brown and D. E. Mayers, Proc. Roy. Soc. (London) **A242**, 89 (1957).
[8] E. Pollard and D. E. Alburger, Phys. Rev. **74**, 926 (1948); D. E. Alburger, Phys. Rev. **73**, 344 (1948).
[9] A. Storruste, Proc. Phys. Soc. (London) **A63**, 1197 (1950).
[10] R. R. Wilson, Phys. Rev. **82**, 295 (1951); **90**, 720 (1953).
[11] W. G. Davey, Proc. Phys. Soc. (London) **A66**, 1059 (1953).
[12] T. D. Strickler, Phys. Rev. **92**, 923 (1953).
[13] J. R. Cook, Proc. Phys. Soc. (London) **A68**, 1170 (1955).
[14] S. Messelt and A. Storruste, Proc. Phys. Soc. (London) **A69**, 381 (1956).
[15] A. K. Mann, Phys. Rev. **101**, 4 (1956).
[16] A. M. Bernstein and A. K. Mann, Phys. Rev. **110**, 805 (1958).
[17] J. S. Levinger, Phys. Rev. **84**, 523 (1951).

Translated by R. Krotkov
193